Design and implementation of a bacterial signaling circuit

Lazova, M.D.

2013

document version
Publisher's PDF, also known as Version of record

Appendix C

Effect of CheB phosphorylation feedback on adaptation kinetics in bacterial chemotaxis

The chemotactic signaling network of bacteria provides a model system for testing the effect of altering network topology on the function of signaling pathways. Here we studied how the disruption of the phosphorylation-dependent feedback via the activity of the methylesterase CheB affects the adaptation kinetics in *Escherichia coli* chemotaxis. Using *in vivo* fluorescence resonance energy transfer (FRET) measurements coupled with temporal step and exponential ramp stimuli, we determined the shape of the transfer function $F(a)$, describing the methylation kinetics of the chemoreceptors, in populations of cells that express a mutant CheB lacking the phosphorylatable N-terminal regulatory domain (CheBc) or having a mutation in the phosphorylation site ($CheB^{D56E}$). We showed that the shape of $F(a)$ differs between wild type cells and cells that express CheBc or $CheB^{D56E}$. $F(a)$ for cells expressing CheBc and having a steady-state kinase activity > 0.40 follows Michaelis-Menten kinetics, whereas a nonlinearity in $F(a)$ of at high values of kinase activity was observed for wild type cells. Our observations suggest that the strong nonlinearity of $F(a)$ could be a consequence of the specific topology of the chemotaxis network of *E. coli*.

Appendix C

C.1. Introduction

Changes in the topology of signaling and regulatory networks can have a strong effect on cellular responses and ultimately the cell fate [134,245]. The simple and thoroughly characterized chemotaxis circuit of *E. coli* [243,266], provides an ideal system for studying the effects of genetic changes of the network topology on the cellular response. In this thesis we have studied the response of a natural chemotaxis network with a different topology by looking at the response functions of the close relative to *E. coli*, *S. typhimurium*, which has an additional scaffolding protein that can be phosphorylated [10] (Chapter 3 and 5). Here, we change the structure of the *E. coli* signaling network by genetic modifications, and using sensitive physiological measurements of the network response, study the consequences of the altered topology *in vivo*.

The bacterial chemotaxis network has a modular structure describable by a coarse-grained model with three dynamic variables: $[L]$ – input (ligand concentration), m – memory (receptor methylation level), and a – output (kinase activity), linked by two transfer functions [260], which have been characterized using FRET experiments [226]. One of the two transfer functions, $G([L],m)$, representing the receptor module, is well described by an MWC model of receptor interactions [260] (see Chapter 3). The second transfer function, $F(a)$, represents the integrand of negative feedback within the adaptation module. It represents the rate of change of receptor methylation, catalyzed by a methyltransferase CheR and methylesterase / deamidase CheB. Assuming that CheR binds only the inactive receptors and CheB – only the active receptors, $F(a)$ can be expressed by an enzymatic reaction model

$$F(a) = V_R \frac{1-a}{K_R+1-a} - V_B(a) \frac{a}{K_B+a}, \qquad (1)$$

where K_R and K_B are the Michaelis constants, and V_R and $V_B(a)$ are the maximal velocities for methylation and demethylation respectively. However, it has been shown experimentally that $F(a)$ could not be fit by a simple mechanistic model of enzyme kinetics [226], as explained below.

$F(a)$ has been mapped experimentally in *E. coli*, using FRET measurements coupled with exponential ramp inputs, $[L](t) = [L]_0 e^{rt}$, where r is the ramp rate, and $[L]_0$ is the ligand concentration, to which the

cells are adapted before applying the ramp [226]. During exponential ramp inputs the kinase activity reaches a new constant steady-state level, a_c, which can be used to infer the shape of $F(a)$ [226] (see Chapter 3, Figure 3.4). For $a < 0.74$, the shape of $F(a)$ can be fit by Michaelis-Menten kinetics, with a constant V_B. As the kinase activity, a, approaches unity, there is a sharp increase in $V_B(a)$, which can be fit by a piecewise linear form (see Chapter 3, equation 22). However, this phenomenological fit does not provide a mechanistic explanation for the strongly non-linear behavior of $V_B(a)$ and $F(a)$ respectively.

One hypothesis for the nonlinearity of $F(a)$ is that it is a consequence of the specific topology of the *E. coli* chemotaxis network, in which CheB activity is controlled by phosphorylation [226]. The methyltransferase CheR and methylesterase / deamidase CheB regulate the level of methylation of the chemoreceptors, which modulates the activity of the receptor-kinase complexes. CheB has a two-domain structure (Figure C.1A). The N-terminal domain is a regulatory (REC) domain, which is phosphorylated by the active kinase (CheA) molecules. The REC domain regulates the activity of the C-terminal domain, which has a methylesterase activity: upon phosphorylation at position D56 in the REC domain, the methylesterase activity is stimulated. The mechanistic explanation of this phenomenon is that in the unphosphorylated CheB, the REC domain packs against the active site of the methylesterase domain, inhibiting its activity (Figure C.1A *left*). Upon its phosphorylation, the REC domain changes its conformation, disrupting the domain interface, which allows access to the methylesterase active site, activating the methylesterase activity of CheB [69] (Figure C.1A *right*). Demethylation of the receptors leads to the deactivation of the receptor-kinase complex, which provides a phosphorylation-dependent negative feedback loop in the chemotaxis system of *E. coli* [15].

To test whether the sharp transition of $F(a)$ around $a = 0.74$ is a result of the phosphorylation-dependent feedback, we transformed Δ*cheB E. coli* cells with plasmids used for expression of mutant CheB variants $CheB^{D56E}$ and CheBc. $CheB^{D56E}$ (Figure C.1B *left*) bears a mutation at the phosphorylation site (D56), which prevents phosphorylation by CheA, *i.e.* the methylesterase activity of $CheB^{D56E}$ cannot be stimulated by

phosphorylation. CheBc (Figure C.1B *right*) is a truncated version of CheB, in which only the methylesterase domain is preserved. It has been shown that CheBc has a much lower methylesterase activity than the phosphorylated intact CheB [69], implying that the phosphorylation of the REC domain has a role not only in the relief of the methylesterase inhibition, but also in the stimulation of the methylesterase activity [15]. If the phosphorylation-dependent feedback on CheB activity is responsible for sharp transition in $F(a)$ at high values of kinase activity, a, observed in wild type *E. coli*, such a sharp transition should not be observed in the $CheB^{D56E}$- and CheBc-expressing strains where the phosphorylation-dependent feedback is disrupted. We describe below our efforts to test this hypothesis using *in vivo* FRET experiments.

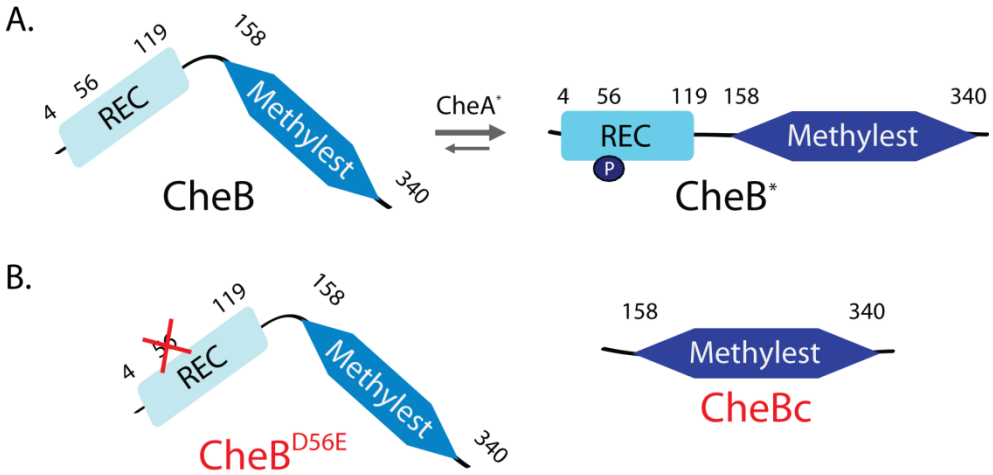

Figure C.1. Domain structure of CheB. (A) CheB has two domains: regulatory (REC) N-terminal domain and methylesterase C-terminal domain. CheB changes its conformation from inactive (*left*) to active (*right*) after phosphorylation of D56 in the REC domain. **(B)** *Left*: $CheB^{D56E}$ is a mutant of CheB, in which the phosphorylation position in the REC domain is mutated and therefore it cannot be phosphorylated. *Right*: CheBc is a truncated mutant of CheB, which lacks the N-terminal REC domain.

C.2. Shape of $F(a)$ in *E. coli* with disrupted phosphorylation feedback, characterized using temporal step stimuli

We characterized the shape of $F(a)$ in Δ*cheB* cells expressing either wild type CheB, CheB^{D56E} or CheBc from an *L*-arabinose-inducible plasmid (see Materials and methods). To measure the rate of change of the methylation level $\frac{dm}{dt} = F(a)$, as a function of the kinase activity a, we used a recently developed experimental strategy, which employs simple step addition and removal of chemoeffector [287]. During adaptation to a step change, in the input ligand concentration, $[L]$, is constant and the methylation level of the receptors, m, changes. Thus, using the model of reference [260], the kinase activity a can be expressed as $\frac{da}{dt} = \frac{da}{dm}\frac{dm}{dt} = \alpha N a(1-a)\frac{dm}{dt}$, where N is the number of ligand binding units in a receptor-kinase complex ($N = 6$ for *E. coli* [260]), and α is the free energy change per methylation increment ($\alpha \approx 2\ k_BT$ for *E. coli* [260]). Therefore $F(a)$ can be expressed as $F(a) = (da/dt)/\left(\alpha N a(1-a)\right)$, and $F(a)$ can be reconstructed experimentally as described below [242].

We applied saturating (1 or 5 mM) steps of α-methyl-aspartate (MeAsp) to wild type cells and Δ*cheB* cells expressing either wild type CheB, CheB^{D56E} or CheBc. We allowed the cells to adapt completely after both addition and removal of MeAsp. We converted the FRET response into units of kinase activity a (see Materials and methods), and calculated da/dt at each point in time by fitting a line to a segment of 31 data points centered at the current time and extracting the slope (the number of data points is consistent with the analysis performed in reference [287]). Using the constants $N = 6$ and $\alpha = 2\ k_BT$ determined previously [226,260], we calculated $\frac{dm}{dt} = F(a)$ and plotted the values as a function of a (Figure C.2A).

In the wild type cells, we observed a steep linear decrease of $F(a)$ at large a, similar to that observed previously in wild type *E. coli* using exponential ramp stimuli [226,287] (Figure C.2A, B). Wild type cells in our measurements had a steady-state kinase activity $a_0 = 0.38$, whereas those in the experiments of reference [226] had $a_0 = 0.33$. The difference in the steady-state kinase activity and the position in which the kink in $F(a)$ occurs ($a \approx 0.62$ in our measurements and $a \approx 0.74$ in the measurements of

reference [226]) might be explained by variations in the expression level of CheB, e.g. due to subtle differences in the growth conditions [192].

In the Δ*cheB* cells expressing CheB from *L*-arabinose-inducible plasmid we controlled a_0 by changing the amount of inducer. By increasing CheB expression level using higher concentration of inducer, we achieved lower a_0 due to the higher demethylation rate at constant expression of CheR. Figure C.2A *left* shows a comparison between wild type *E. coli*, and Δ*cheB E. coli*, complemented with CheB using 0.0001% and 0.0003% *L*-arabinose as an inducer, having a_0 of 0.38, 0.46 and 0.34 respectively. For all three strains we could not fit the entire $F(a)$ using the the Michaelis-Menten model of equation (1) with a constant maximal rate of demethylation V_B: a steep linear decrease occurs at $a \approx 0.62$, 0.60 and 0.72 respectively (Figure C.2A *left*).

We measured the shape of $F(a)$ in Δ*cheB* cells expressing CheBc and $CheB^{D56E}$. Cells expressing CheBc with a kinase activity of 0.48 and 0.42 (CheB expression induced with 0.0001% and 0.0003% *L*-arabinose respectively) can be fit by equation (1) with a constant V_B (Figure C.2A *middle*). Δ*cheB* cells expressing $CheB^{D56E}$ (0.00015% *L*-arabinose, $a_0 = 0.42$), as well as cells, expressing larger amounts of CheBc (0.001% *L*-arabinose, $a_0 = 0.20$), both showed a kink in $F(a)$ at $a \approx 0.85$ (Figure C.2A *right* and *middle*) and thus cannot be fit by equation (1) with a constant V_B.

C.3. Shape of *F(a)* in *E. coli* with disrupted phosphorylation feedback, characterized using exponential ramp stimuli

We confirmed the difference in the shape of $F(a)$ in cells that express CheBc by measuring the constant kinase a_c activity reached during temporal exponential ramp stimulation, and converting the obtained gradient senitivity curve to $F(a)$ (see Chapter 3). Figure C.2B shows the results obtained using FRET measurements in CheBc-expressing cells (0.0003% *L*-arabinose, $a_0 = 0.42$), in comparison to results from the same type of measurements in wild type cells taken from reference [226]. Similar to the result from the analysis of the response to a step, $F(a)$ for CheBc-expressing cells could be fit by equation (1) with a constant V_B (Figure C2.B). Thus, we conclude that the phosphorylation-dependent feedback in wild

type *E. coli*, which is disrupted in CheBc cells, affects the shape of $F(a)$ at high levels of kinase activity.

Table C.1 summarizes the fitted parameters for the Michaelis-Menten model (equation (1)) for all strains shown of Figure C.2A and B.

Strain	a_0	V_R (s^{-1})	V_B (s^{-1})	K_R	K_B	a in which a kink in $F(a)$ occurs
WT	0.38	0.008	0.007	0.32	0.30	0.62
CheB	0.46	0.008	0.006	0.32	0.30	0.72
CheB	0.34	0.008	0.008	0.32	0.30	0.60
CheBc	0.46	0.008	0.007	0.32	0.08	-
CheBc	0.42	0.008	0.006	0.32	0.08	-
CheBc	0.20	0.008	0.008	0.32	0.08	0.85
CheB^{D56E}	0.42	0.014	0.009	0.32	0.01	0.85
WT	0.33	0.010	0.013	0.32	0.30	0.74
CheBc	0.42	0.014	0.013	0.32	0.08	-

Figure C.1. Fitted parameters to the data shown on Figure C.2, using equation (1). Fits to equation (1) end at the value of a, shown in the last column. CheB, CheB and CheB^{D56E} refer to Δ*cheB* strains, expressing the respective CheB variant from a plasmid. The last two rows refer to the strains, used in Figure C2.B. Note that the fits are not well constrained.

Appendix C

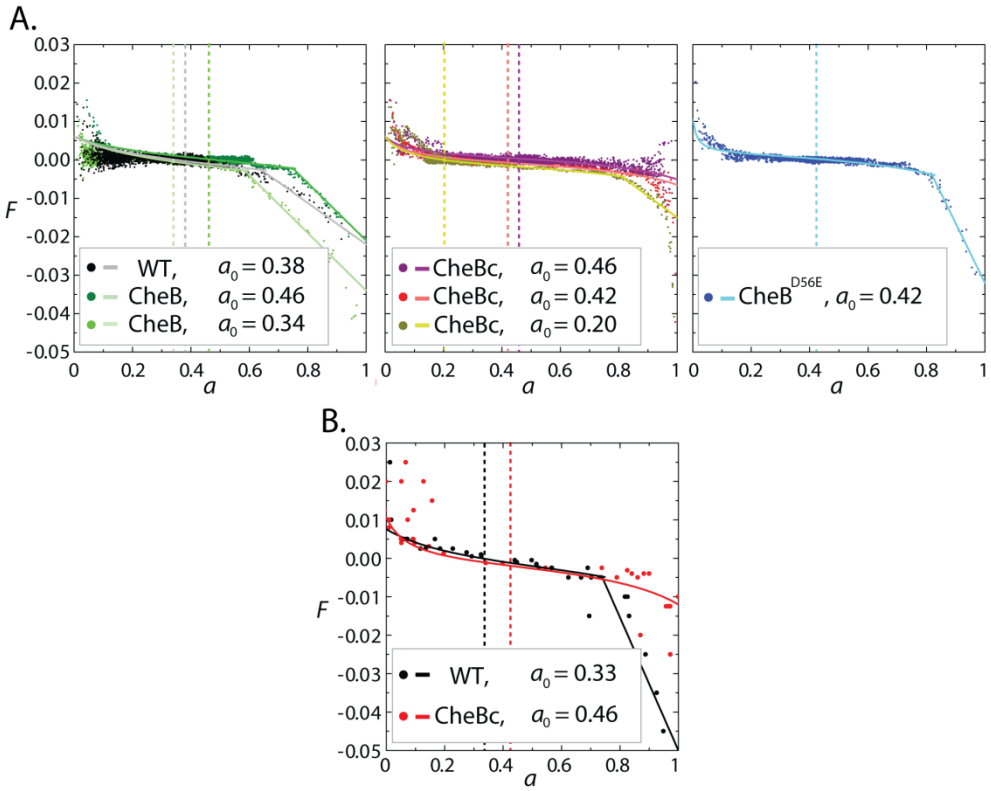

Figure C.2. Effect of disruption of the phosphorylation-dependent feedback in bacterial chemotaxis on the shape of *F*(*a*). The shape of $F(a)$ was determined using step stimuli **(A),** and exponential ramp stimuli **(B)**. Results for strains expressing CheB (left), CheBc (middle), and CheB^{D56E} (right) are shown with the name of the CheB variant within each panel. Different colors of each panel in (A) correspond to different induction levels of the CheB variants, leading to different a_0 (indicated within the key of each panel, and with a vertical dashed line). The result for wild type (WT) *E. coli* is shown for comparison in the left panel of (A). The data for wild type *E. coli* shown in (B) is taken from reference [226]. Fits with Michaelis-Menten model are shown for all strains with parameters, indicated in Table C.1. Linear fits are shown for the segments that could not be fit by the Michaelis-Menten model.

C.4. Discussion

A fundamental question in systems biology is how the topologies of biochemical networks affect their input-output relationships, *i.e.* transfer functions [22,280]. We have shown an example of how *in vivo* FRET measurements can be used to elucidate the effect of topological changes in a biological signaling circuit. We used *E. coli* cells in which the chemotaxis system was genetically altered in such a way that removes the phosphorylation feedback on the methylesterase activity of CheB, *i.e.* cells, expressing a CheB mutant with a disrupted phosphorylation site ($CheB^{D56E}$) or lacking the phospho-receiver domain (CheBc). Using FRET measurements coupled with temporal step and exponential ramp stimuli, we demonstrated that in contrast to wild type cells, the transfer function $F(a)$ of CheBc-expressing cells with a steady-state kinase activity > 0.40 can be fit by Michaelis-Menten kinetics with a constant maximal rate of demethylation V_B (Figure C.2). CheBc-expressing cells with lower steady-state kinase activity ($a_0 = 0.20$), as well as Che^{BD56E}-expressing cells (with $a_0 = 0.42$) showed a steep linear decrease of $F(a)$ at high values of a similar to that observed in wild type cells (Figure C.2). CheBc has a much lower methylesterase activity than the phosphorylated intact CheB [69], and $CheB^{D56E}$ cannot be activated by phosphorylation, implying that the higher activity of CheB induced by the phosphorylation feedback leads to the nonlinearity of $F(a)$ at large a.

The mechanistic event that determines the characteristic kink of $F(a)$ in wild type *E. coli* cells is still to be identified. Clausznitzer et al. [56] propose that the fast demethylation at high a could be due to cooperative action of two phosphorylated CheB (CheB-P) molecules: one CheB-P molecule could bind to a C-terminal tether of a chemoreceptor to allosterically activate the group of surrounding chemoreceptors, while another CheB-P molecule demethylates the activated chemoreceptors [23,56]. A plausible explanation of the effect of the phosphorylation feedback is that the phosphorylation of CheB affects its association with the receptor-kinase clusters, and its proximity with its substrate (chemoreceptors) and phosphorylation enzyme (CheA) respectively. Imaging of fluorescently labelled CheB and CheBc showed that they both localize to the cell poles but CheBc localizes to a

lesser extent [20]. The dynamic localization of CheB with the receptor clusters can be further assessed using superresolution microscopy imaging in living cells, such as photoactivated localization microscopy (PALM) [94].

A form of CheB similar to CheBc might exist in wild type bacteria. Simms et al. [233] reported that purified CheB from *S. typhimurium* contains two forms of CheB: the intact full-length product of *cheB* gene and a C-terminal fragment, starting at residue 147 of the intact CheB, *i.e.* containing the full methylesterase domain (see Figure C.1). The C-terminal fragment could be a result of proteolysis of the full-length CheB, which is a common mechanism for turning on enzymatic activities [53,108,187]. This fragment itself could target to the receptor-kinase clusters [20]. The ratio of full-length to C-terminal fragment of CheB in wild type cells could affect the shape of $F(a)$ and the position, in which the steep decrease of $F(a)$ occurs.

Another explanation could lie in the cell-to-cell variation of the expression of CheR and CheB in *E. coli* cells (Ned Wingreen, personal communication; Michael Salazar's B.Sc. thesis, 2010). The net rate of receptor methylation is proportional to the methylation rate of CheR, v_R, minus the demethylation rate of CheB, v_B, assuming for simplicity linear, rather than Michaelis-Menten kinetics, and that only the inactive receptors are methylated and only the active receptors are demethylated:

$$F(a) = \frac{dm}{dt} = v_R(1-a) - v_B a, \qquad (2)$$

where v_R and v_B are the rate constants of CheR and CheB respectively. For temporal exponential ramp stimuli with ramp rates r, it has been shown that $F(a) = r/\alpha$, where α is the free energy added to the free energy of the receptor-kinase complex per methylation increment [226] (see Chapter 3). Thus, for equation (2) it follows that

$$a_c = \frac{v_R}{v_R+v_B} - \frac{1}{\alpha(v_R+v_B)} r, \qquad (3)$$

where a_c is the constant kinase activity reached during ramp stimulation. Assuming that for individual cells v_R and v_B are constants, for $0 < a < 1$ the gradient-sensitivity curve $a_c(r)$ is a straight line, and it becomes constant when a_c reaches 0 or 1, its minimum and maximum respectively. However, different cells in a bacterial population produce different amounts of CheR and CheB: it has been reported that the steady-state distributions of protein concentration in a population of cells generally follow a gamma

distribution as a consequence of the stochastic protein expression [85]. The v_R and v_B values will be large for cells producing large amounts of CheR and CheB, therefore the slope of $a_c(r)$ will be shallow (see equation (3)), and a_c will reach 1 at large values of r. The opposite will be observed for cells expressing small amounts of CheR and CheB, therefore a_c will reach 1 at small values of r. Salazar et al. simulated the effects of such variability in adaptation kinetics at the population level, and found that the cell-to-cell variations in v_R and v_B values can lead to the sharp nonlinearity in $a_c(r)$ observed experimentally [226] even if $F(a)$ for each cell is a linear function of a. The shape of the feedback trasfer function $F(a)$ can be obtained from the $a_c(r)$ curve by inverting $a_c(r) = F^{-1}(r/\alpha)$ [226,260], thus the strong nonlinearity in $a_c(r)$ could explain the kink in $F(a)$. This hypothesis could be tested experimentally by observing the shape of $F(a)$ in single cells.

Future developments of sensitive physiological assays comparable to these FRET measurements of the chemotaxis pathway, for other biological signaling systems could shed light on the function of regulatory motifs that can be genetically altered. Considering biological sensory systems as modular structures, knowledge of the function of particular cellular regulatory motifs could accelerate the development of bioengineering and synthetic biology [51,200].

C.5. Materials and methods

Bacterial strains and plasmids

The FRET donor–acceptor pair (CheZ-CFP and CheY-YFP) was expressed from a plasmid pVS88 [240] in a Δ*cheB* Δ*cheY* Δ*cheZ E. coli* RP437 (*i.e.* VS124, gift from Victor Sourjik). Wild type *cheB*, non-phosphorylatable mutant *cheB*^{D56E} and truncated mutant *cheBc* (containing the last 612 base pairs of *cheB*) were cloned into pBAD33 vector using SacI and XbaI cloning sites (pVS91, pVS97 and pVS112 plasmids respectively, gifts from Victor Sourjik). The expressions of wild type CheB, CheB^{D56E} and CheBc were induced with *L*-arabinose (the percentages of *L*-arabinose that we used for the different plasmids and experiments are indicated in the text). Wild type

Appendix C

E. coli refers to Δ*cheY* Δ*cheZ E. coli* RP437 expressing CheY-YFP and CheZ-CFP from pVS88.

In vivo *FRET measurements and data analysis*

Cells were grown at 250 rpm at 33.5°C in a rotary shaker to mid-exponential phase (OD_{600} ~ 0.5) in tryptone broth (TB; 1% tryptone, 0.5% NaCl, pH 7.0) supplemented with appropriate antibiotics and inducers. Cells were harvested by centrifugation, washed twice and resuspended in motility buffer (10 mM potassium phosphate, 0.1 mM EDTA, 1 μM methionine, 10 mM lactic acid, pH 7), and stored at 4°C for 1-5 h prior to the experiment.

FRET microscopy of bacterial populations was performed as described previously [242]. Cells, attached to a poly-*L*-lysine-coated coverslip, were situated at the top face of a bespoke flow cell [27], and kept under constant flow of motility buffer, generated by a peristaltic pump (Rainin Dynamax RP1) or syringe pump (Harvard Apparatus, PHD2000). Exponential ramp stimuli were generated by mixing a concentrated solution of the chemoeffector α-methyl-*DL*-aspartate (MeAsp; Sigma Aldrich) and motility buffer by a fluid mixer of a type described before [35,226] (see Chapter 3). An upright microscope (Nikon FN1) was equipped with an oil immersion objective (Nikon CFI Plan Fluor, 40x/1.3). The sample was illuminated by a metal halide arc lamp with closed-loop feedback (EXFO X-Cite *exacte*) through an excitation bandpass filter (Semrock, FF01-438/24-25) and a dichroic mirror (Semrock, FF458-Di01). The epifluorescent emission was split by a second dichroic mirror (Semrock, FF509-FDi01) into donor (cyan, *C*) and acceptor (yellow, *Y*) channels and collected by two photon-counting photomultipliers (Hamamatsu H7422P-40) through bandpass filters (Semrock FF01-483/32 and FF01-542/27 for the *C* and *Y* channels, respectively). Detector output from the two channels were recorded through a data acquisition card (National Instruments) installed on a PC running custom-written software.

After background subtraction, the ratio between the acceptor and donor channel ($R = Y/C$) was used to compute the change in FRET efficiency upon stimulation (see Chapter 3). Under the conditions of the

measurements, $\Delta FRET \sim \Delta R$, and we expressed $\Delta FRET$ for simplicity in arbitrary units of ΔR.

$\Delta FRET(t)$ was normalized to the absolute magnitude of the response to addition of a saturating attractant step, $\left|\Delta FRET_{sat}^{add}\right|$, to compensate for variations due to different absolute levels of signal between the experiments. The steady-state kinase activity, a_0, was calculated as $a_0 = \frac{\left|\Delta FRET_{sat}^{add}\right|}{\left|\Delta FRET_{sat}^{add}\right|+\left|\Delta FRET_{sat}^{remove}\right|}$, where $\Delta FRET_{sat}^{remove}$ is the response to removal of a saturating attractant step after the cells have been completely adapted. The kinase activity $a = a_0 + \Delta a$, where $\Delta a = \frac{\Delta FRET}{\left|\Delta FRET_{sat}^{add}\right|+\left|\Delta FRET_{sat}^{remove}\right|}$ is the kinase activity change in every point in time.

C.6. Acknowledgements

The work with CheB mutant strain was performed by Quyen Le, a M.Sc. student (University of Twente).

Appendix C